Turbulent Dispersion in a Pipe Flow

H. A. BECKER
Queen's University, Kingston, Ontario, Canada

R. E. ROSENSWEIG
AVCO Corporation, Wilmington, Massachusetts

J. R. GWOZDZ
Massachusetts Institute of Technology, Cambridge, Massachusetts

The nearly homogeneous, isotropic turbulence field in the core of a fully developed pipe flow was chosen as the medium for turbulent dispersion of a smoke tracer injected from a point on the centerline. By using the optical probe technique the fields of the mean and fluctuating point concentration were mapped at several Reynolds numbers, and spectral analyses made of concentration fluctuations on the plume axis. With the use of sheet illumination, the mean and fluctuating components of the integral material concentration in a plume cross section were measured and the fluctuating component was spectrally analyzed. The maximum Reynolds number was 684,000, the maximum ratio of root-mean-square concentration fluctuation to mean concentration exceeded 100% for points and 40% for sheets, and the turbulent Peclet number was found to equal 850. The existence of standard flow conditions was confirmed by measurement of the frictional drag coefficient and the mean concentration field.

The turbulent dispersion of matter released from a point source can be described (*1, 2*) by the superposition of two processes: (1) turbulent motions small in scale relative to the material could cause the material to spread about the instantaneous center of gravity, and (2) large-scale turbulent motions cause meandering (aimless wandering) of the instantaneous center of gravity. In small dispersion times t, dispersion is due mostly to meandering, and Taylor's theory of single-particle diffusion (*3*) predicts that the mean-square displacement $\overline{y^2}$ of material from the time-mean center of gravity is proportional to the square of the dispersion time t^2. For dispersion effected by turbulence concentrated within an equilibrium convection subrange, the similarity theory of turbulent dispersion predicts that the mean-square displacement $\overline{Y^2}$ from the *instantaneous* center of gravity is proportional to the cube of the dispersion time t^3, a relation first suggested by Richardson (*4*) and known as Richardson's law. Lin (*5*) has recently derived Richardson's law from a kinematic analysis of two-particle turbulent dispersion. It is, of course, physically necessary that $\overline{y^2}$ and $\overline{Y^2}$ eventually converge to a limiting ratio. For large dispersion times, both $\overline{y^2}$ and $\overline{Y^2}$ are expected to, and Taylor's theory predicts that, $\overline{y^2}$ will vary linearly with time: $\overline{y^2}$ or $\overline{Y^2} \propto t - t_o$, where t_o is the virtual temporal origin of the final period.

The predictions of Taylor's theory have been amply confirmed by experiment (*6*), while observations of oceanic (*7*) and atmospheric (*8*) turbulent dispersion have supported the validity of Richardson's law. It seems, however, that further progress could be made by study of Richardson diffusion in a well-characterized laboratory turbulence. It turns out that the generation of a well-characterized, laboratory-scale turbulence in which the meandering process is detectable is a challenging problem. The emphasis of the present study concerns the more usual laboratory regime in which the meandering of the center of gravity is small in comparison to the dispersion about the center of gravity, for even in this our factual knowledge is very small.

The statistical theories of Taylor and Lin result in predictions for the mean concentration field in a turbulent diffusion plume but cast no light on the turbulent concentration fluctuations. An attempt along these lines is the fluctuating plume model of Gifford (*2*) which attempts to predict concentration fluctuations by attributing these to the meandering of an otherwise stationary concentration pattern. This is only a partial approximation to reality, and what the model neglects may be more important than the effect it accounts for. Gifford's basic assumption must therefore be experimentally validated before his theory can be accepted; that is, it must be demonstrated that meandering is a sufficiently large effect to account alone for the bulk of the concentration fluctuation occurring at a point.

Published data on scalar fluctuations of an injected species in gaseous systems are rather fragmentary. Among the available data are those of Corrsin and Uberoi (*9*), who made measurements at a few points downstream of a line source of heat in a turbulent jet of air. Rosensweig (*11, 12*) developed a scattered-light technique for studying the concentration field of suspended colloidal particles marking one of the fluid streams entering a mixing field. A linear response is obtained to both the time-mean and the time-variant components of material concentration at a point, in a sheet, or in a volume, according to the modes of illumination and observation. In particular, turbulent concentration fluctuations can be accurately detected and electronically analyzed. Rosensweig investigated turbulent mixing between a free jet of air (marked by an oil fog) and the clear ambient air. Becker (*13* to *15*) subsequently studied jet mixing on a confined jet system, while Forslund and Sargent (*21*) devoted further study to the mixing of a jet.

In the present study the nearly homogeneous, isotropic turbulence field in the core of a fully developed pipe flow was chosen as the medium for the turbulent dispersion of a tracer injected from a point on the center line. The fields of the mean and root-mean-square fluctuating point concentration were mapped at several Reynolds numbers, and spectral analyses were made of point concentration fluctuations on the plume axis. With the use of sheet illumination, measurements were also made of the mean and fluctuating components of the integral material concentration in a plume cross section, and the fluctuating component was spectrally analyzed.

THE SCATTERED-LIGHT TECHNIQUE

The scattered-light technique is a method for studying mixing between streams by marking one of these with a sol (a suspension of colloidal particles) and using the light-scattering property of the sol to detect the material of the marked stream. The principle is simple: The zone of a mixing field within which it is desired to detect the quantity of the marking sol is uniformly illuminated and light scattered from the volume of interest (usually at right angles to the incident beam) is focused on a photocell. The photocell gives a signal linear in the instantaneous content of sol M, assuming, as is normally true, that the characteristics of the sol particles are invariant over the field where Γ is the point concentration of sol and V is the volume of interest. The signal is then analyzed electronically; for example, a d.c. voltmeter gives the time-mean material content $\overline{M}$:

$$\overline{M} \equiv \lim_{T\to\infty} \frac{1}{T} \int_t^{t+T} M dt$$

The detection of point concentrations requires the use of a small-diameter beam of light. A lens viewing the beam at right angles focuses the scattered light on a slitted diaphragm, forming thereon an image of the incident beam. The slit passes the light scattered from a short segment of the incident beam to a photocell. That segment then defines the volume observed. When the observed volume is sufficiently small, the photocell signal is directly proportional to the instantaneous point concentration, that is

$$\lim_{V\to 0} \int_V \Gamma dV \equiv \Gamma V$$

The criteria for sufficient smallness of the observed volume are now well known (*11, 12, 15*).

Measurement of the material concentration in a cross section of a flow

$$\Omega \equiv \int_A \Gamma \, dA$$

where A is the area viewed, requires the use of a uniform sheet of light. At a distance from the sheet-illuminated mixing zone sufficiently great so that differences in optical path length are effectively negligible, scattered light is gathered by a lens and focused on a photocell. When the observed layer is thin enough, the signal is directly proportional to Ω.

THE APPARATUS

The Pipe

The pipe was a 90-diameter-long straight run of 8-in. nominal diameter aluminum irrigation piping. The true I.D. was 20.1 cm., based on the inside circumference. Straightening vanes and calming screens were provided at the inlet. The 90-diameter length was judged sufficient for a very close approach to equilibrium flow over the final six diameters of length which constituted the test section.

In operation, longitudinal traverses of the diffusion plume were made by observing a fixed cross section of the flow and by varying the position of the oil fog injector, not vice-versa. To ease the problem of optical observation, the cross section of interest was located, not inside the pipe, but 5 cm. beyond its end; experience with jets showed that the core flow pattern would suffer no measurable change over this short distance. The pipe was tapped for insertion of the oil fog injector at intervals of 5.1 cm. (2 in.) over the final six diameters of length.

Fog Injectors

Two fog injectors were made of 12-gauge hypodermic tubing (2.77 mm. O.D., 2.16 mm. I.D.). These injected oil fog at the local mean velocity of the pipe flow. Ideally, such an injector should be vanishingly small in order not to perturb the flow. In practice, however, the injector had to provide a sufficiently copious flow of fog to raise fog concentrations in the diffusion plume to a level high enough for proper use of the scattered-light technique.

Injector A was designed for the injection of fog on the axis of the pipe and was streamlined for minimum disturbance of the flow. Injector B was built later, when it was undertaken to make radial traverses of the diffusion plume. It would have been expensive in arrangement and clumsy of execution to traverse the flow radially with the light-scatter equipment. The simpler alternative of moving the fog injector across the diameter of the flow and holding the point of observation fixed on the axis was therefore chosen and injector B was designed for this purpose.

Oil Fog Generator

The oil fog generator described by Becker (*13*) was used. In this generator, a hydrocarbon oil (Esso's Coray 55) of narrow molecular weight range and with an average molecular weight of about 300 is evaporated into a hot stream of air. The air-vapor mixture is then rapidly cooled, forming the oil fog.

ESTIMATE OF ACCURACY

The only source of inaccuracy worthy of a detailed examination is the disturbance of the pipe flow by the fog injectors.

The pressure drop occasioned by the streamlined injector A was not detectable. The nonstreamlined injector B was equal in effect (when centered on the pipe axis) to a half-diameter length of pipe. The turbulence generated by injector B can be roughly characterized: The mean-square maximum velocity fluctuation downstream of an infinite cylinder in a uniform stream is approximately $\overline{u^2} = 0.07\ U^2 D_{cyl}/x$, where D_{cyl} is the cylinder diameter. At a distance of 100 cylinder diameters, the fluctuation is of about the same intensity as in the core of a pipe flow, $\overline{u^2} \approx 0.0008\ U^2$. In the present system, 100 cylinder diameters were equivalent to 1½ pipe diameters.

The disturbing effect of the injector could be large only very near the source. The present measurements were begun at a distance of about three pipe diameters from the source. The differences between the actual data at this distance and those that would have been obtained with a truly passive source are probably measurable but not serious.

RESULTS

Pipe Flow Parameters

Measurements of the frictional pressure drop were made at pipe Reynolds numbers $N_{Re} \equiv D_p U_{av}\, \rho/\mu$ of 481,000 and 684,000. The values for the average velocity of discharge U_{av}, the friction factor $f \equiv D_p(dp/dx)/\frac{1}{2}\rho U_{av}^2)$, and the friction velocity $u^* \equiv \sqrt{\tau_o/\rho}$ are summarized in Table 1. The pressure drops were about 10% higher than would occur in a perfectly smooth pipe, and the friction factors indicate a relative pipe roughness of 0.00007.

The Field of the Mean Point Concentration

The field of the mean point concentration of material in a diffusion plume generated by a point source in the core of a pipe flow has been studied by numerous investigators (*6, 16* to *19*). The present data may be better than any previously obtained, owing to the advantages of the scattered-light technique.

TABLE 1. FLOW PARAMETERS CALCULATED FROM THE CENTERLINE VELOCITY AND THE FRICTIONAL PRESSURE DROP

N_{Re}	f	$U_{av}/\overline{U}_c$	$u^*/\overline{U}_c$
481,000	0.01397	0.8567	0.186
684,000	0.01357	0.8587	0.184

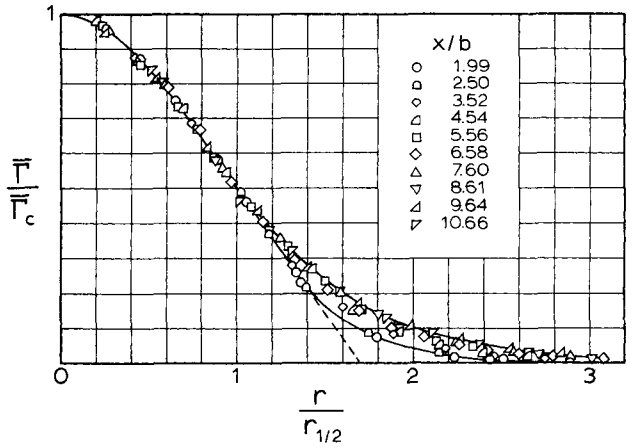

Fig. 1. Radial profiles of the point concentration at a Reynolds number of 684,000 (centerline velocity 61 meters/sec.).

Several pipe Reynolds numbers were investigated, the highest being 684,000. This maximum Reynolds number is about 10% higher than has previously been realized in such experiments and, according to the data compiled by Hanratty, Kada, and Flint (*17*), is certainly high enough to assure location within the regime of Reynolds number's independence of the turbulent material diffusivity.

The radial concentration profile in a diffusion plume is normally bell-shaped and is characterizable as to scale by two amplitudes: the central maximum of the concentration $\bar{\Gamma}_c$, and the radius $r_{1/2}$ at which the concentration is one-half the maximum. In the event of self-preservation (that is, invariance under downstream translation), $\bar{\Gamma}/\bar{\Gamma}_c$ is a unique function of $r/r_{1/2}$:

$$\bar{\Gamma} = \bar{\Gamma}_c \cdot g(r/r_{1/2})$$

More generally, however, the distribution function g depends on the distance from the source, At small values thereof, g is also a function of the pipe Reynolds number.

Figure 1 shows a normalized representation of the data for the highest Reynolds number, 684,000. The profiles are self-preserving up to $r = r_{1/2}$. Beyond this point, they become narrower-skirted with increasing distance from the source. The data for large radii are better seen in a semilogarithmic representation, Figure 2. The self-preserving core is exactly described by the normal distribution function

$$\bar{\Gamma} = \bar{\Gamma}_c \exp\{-0.693\ (r/r_{1/2})^2\}, \quad r < r_{1/2} \qquad (1)$$

At larger radii the data diverge and no limiting form appears to be approached either near to or far from the source. In the case of a truly homogeneous, isotropic field of turbulence translated past the point of observation at a uniform velocity, self-preservation should be asymptotically approached far downstream of the source.

It should be remembered that the present profiles were obtained by moving the source across a pipe diameter while holding the point of observation fixed on the axis. Hence the radius r here measures distance from the center of the resulting profile, not from the axis of the pipe. Had the mean velocity been radially uniform and the turbulence fully homogeneous and isotropic, there would have been no difference between this and the converse mode of traversing. In the actual experiment, there should be no practical difference up to at least $r = b/2$. The maximum value of the plume half-radius $r_{1/2}$ in Figures 1 and 2 is approximately ¼ of the pipe radius. Within this distance from the center of a pipe flow at a Reynolds number of 700,000, the mean velocity does not change by more than 3% of the centerline value, nor do the turbulence properties affecting diffusion vary significantly. Hence turbulent diffusion at $r < b/2$ was, in effect, affected only by the centerline mean velocity U_c and the centerline turbulence properties. The absence of a tendency toward self-preservation at the skirts of the concentration profile at large distances from the source can be attributed largely to the increasing penetration, as the pipe wall is approached, of regions exhibiting pronounced radial variation of the mean velocity and of the turbulence properties affecting diffusion.

The mean-square material displacement from the plume centerline is

$$\overline{r^2} \equiv \frac{\int_0^\infty r^2 \bar{\Gamma}\, d(\pi r^2)}{\int_0^\infty \bar{\Gamma}\, d(\pi r^2)}$$

For the normal distribution [Equation (1)], $\overline{r^2}$ is related to the half-radius $r_{1/2}$ by the proportionality

$$\overline{r^2} = r_{1/2}^2/0.693 \qquad (2)$$

Equation (2) applies, to a fair approximation, to the present data; the departures from the normal distribution occurring at the fringes of the diffusion plume cannot easily be held account of and, for large distances from the source, are properly ignored if interest is restricted to the core region of the pipe flow in which the mean velocity was essentially constant and the turbulence nearly homogeneous and isotropic. With the use of Equation (2). the parameters in Taylor's statistical theory of one-particle diffusion are easily evaluated. The theory gives for one component of mean-square material displacement the relations

$$\overline{y^2} = \overline{v^2}\ t^2 \qquad (3)$$

for small diffusion times and

$$\overline{y^2} = 2\,\overline{v^2}\,T_L(t - t_o) \qquad (4)$$

for large diffusion times, where v is the y component of fluctuation in the particle velocity, T_L is the integral time scale of the particle motion (called the *Lagrangian time scale*), and t_o is the virtual temporal origin of the final period of diffusion. For an axisymmetrical diffusion plume, v is the radial component of particle velocity and $\overline{y^2} = \frac{1}{2}\,\overline{r^2}$. For a turbulence field translated past the diffusion source at high velocity (that is, $\bar{U} >> v$, fully realized in the core of a pipe flow), $t = x/U$. The Lagrangian integral time scale T_L can be expressed in terms of the Lagrangian integral length scale Λ_L as $T_L = \Lambda_L/v$. With

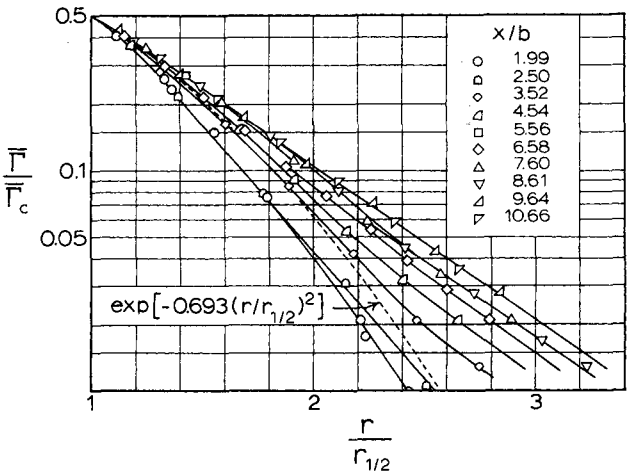

Fig. 2. Radial profiles of the point concentration in the outer portion of the plume (data of Figure 1 replotted).

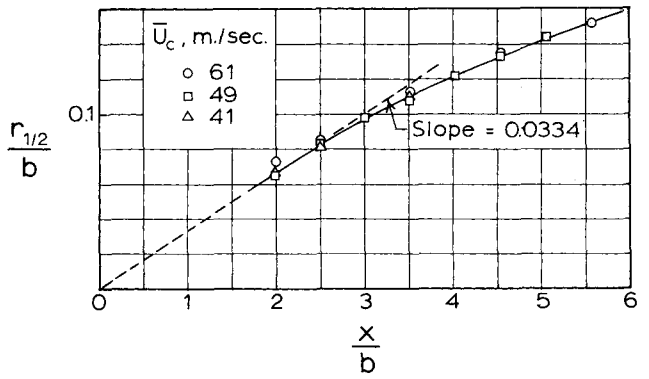

Fig. 3. The concentration half-radius of the plume as a function of distance from the source.

these substitutions, Equations (3) and (4) give for the present case

$$r_{1/2}^2 = 2(0.693)\,\overline{v^2}\; x^2/\bar{U}_c^2 \qquad (5)$$

for the neighborhood of the source and

$$r_{1/2}^2 = 4(0.693)\,\hat{v}\Lambda_L(x - x_o)/\bar{U}_c \qquad (6)$$

for the domain far downstream. Here $\hat{v}\Lambda_L(= \overline{v^2}\; T_L)$ is identical with the turbulent material diffusivity $\mathcal{D}_T$.

Figure 3 shows $r_{1/2}/b$ as a function of x/b for the neighborhood of the source. The linearity predicted by Equation (3) is not demonstrated, owing to the absence of data very near the source (a closer approach to the source was not practical with the present apparatus; a micrometer screw would have been needed to position accurately the fog injector. In any case, data for the region very near the source would have been of dubious significance, owing to the finite initial size of the plume and to the disturbance of the equilibrium pipe flow by the fog injector). A tangent to the data, produced from the source (assuming the effective origin to be coincident with the source), should, it appears, have a slope closely approximating $\sqrt{1.386}\;\hat{v}/\bar{U}_c$. The relative intensity of the radial fluctuation in the velocity of a diffusing particle is thus estimated to be $\hat{v}/\bar{U}_c = 0.0284$. Baldwin and Walsh (*16*) studied diffusion of heat from a line source in air flow through a 20-cm. (8 in.) nominal diameter commercial pipe 45 diameters long at mean velocities of 22, 32, 41, and 49 meters/sec. and estimated values of $\hat{v}/\bar{U}_c$ of 0.027, 0.029, 0.028, and 0.032. The agreement

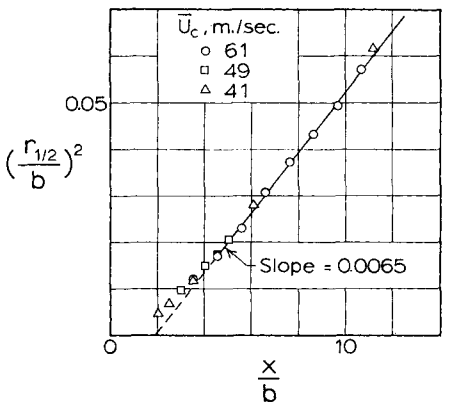

Fig. 4. The square of the concentration half-radius as a function of distance from the source.

with the present result is very close and is certainly within the probable experimental error.

Figure 4 shows $(r_{1/2}/b)^2$ as a function of x/b. The linearity predicted by Equation (6) for the far downstream regime is well realized. The spatial origin of the final period lies 1.95 pipe diameters downstream of the source. From the slope, 0.0065, it is estimated that $\hat{v}\Lambda_L/\bar{U}_c b = 0.00235$. On substituting the value 0.0284 for $\hat{v}/\bar{U}_c$, this gives for the Lagrangian spatial scale $\Lambda_L = 0.083\; b$. Since $\hat{v}\Lambda_L$ is the turbulent material diffusivity, we have for the turbulent Peclet number N_{Pe} ($\equiv D_p\bar{U}_c/\mathcal{D}_T$) $= 2/0.00235 = 852$. Baldwin and Walsh (*16*) obtained an average value of 910. Towle and Sherwood's data (*19*) on material diffusion in air indicate $N_{Re} = 850$ at high Reynolds numbers. The data of Flint (*17*) on air and Kada (*17*) on water, however, indicate a value of 1,250. Mickelson's data (*18*) on air scatter between 800 and 1,200. The present data were obtained with less disturbance of the pipe flow by both the source and the detection device than in any previous work (the optical probe indeed caused no disturbance whatever). Hence the value of $N_{Pe} = 850$ can probably be regarded as definitive. It should be noted that the present data pertain to the case of a diffusing material (submicron size oil droplets) with a negligible molecular diffusivity. In the case of hydrogen in air, molecular diffusion is quite significant, and Flint (*17*) calculated turbulent diffusivities from his data by assuming that turbulent and molecular diffusion are additive processes motivated alike by the mean concentration gradient.

The turbulent material diffusivity is constant, according to Taylor's theory (*3*), only in the final period of diffusion when the instantaneous and the initial particle motions are no longer correlated in any significant degree. A solution of the classical gradient diffusion equations for a constant diffusivity and constant mean velocity gives for the present case (*6*)

$$\bar{\Gamma} = \frac{J}{4\pi\mathcal{D}_T\sqrt{x^2 + r^2}}\exp\left\{-\frac{U_c\,(\sqrt{x^2 + r^2} - x)}{2\mathcal{D}_T}\right\} \qquad (7)$$

where J is the source strength. Near the x axis, $r << x$ and $\sqrt{x^2 + r^2} = x(1 + r^2/x^2)^{1/2} \approx x + \frac{1}{2}\, r^2/x$, giving

$$\bar{\Gamma} \approx (J/4\pi\,\mathcal{D}_T\,x)\,\exp\{-U_c\,r^2/4\,\mathcal{D}_T\,x\} \qquad (8)$$

On the axis

$$\bar{\Gamma} = \bar{\Gamma}_c = J/4\pi\,\mathcal{D}_T\,x \qquad (9)$$

The radial concentration distribution near the axis can therefore be written

$$\bar{\Gamma} \approx \bar{\Gamma}_c\exp\{-U_c\,r^2/4\,\mathcal{D}_T\,x\} \qquad (10)$$

Comparison with Equation (1) then gives

$$r_{1/2}^2 = 4(0.693)\,\mathcal{D}_T x/\bar{U}_c \qquad (11)$$

On locating the origin of x at the virtual origin x_o of the final diffusion period, this relation is seen to be identical with that [Equation (6)] obtained from Taylor's theory. In accord with the present experimental results, the gradient diffusion model predicts that the radial concentration

TABLE 2. CONSTANCY OF THE PRODUCT $\bar{\Gamma}_c r_{1/2}^2$ AT $N_{Re} = 684{,}000$

x/b	1.99	3.01	3.52	4.53	5.56	6.58	7.60	8.61	9.64	10.7
$\bar{\Gamma}_c\, r_{1/2}^2$	1.03	1.03	1.00*	0.98	0.99	1.05	0.98	0.97	0.95	1.01

* Reference value.

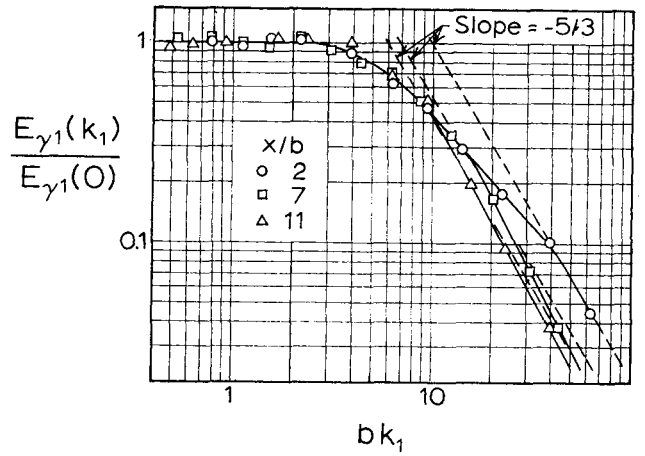

Fig. 5. Spectra of point concentration fluctuations on the plume (and pipe) axis at a Reynolds number of 450,000.

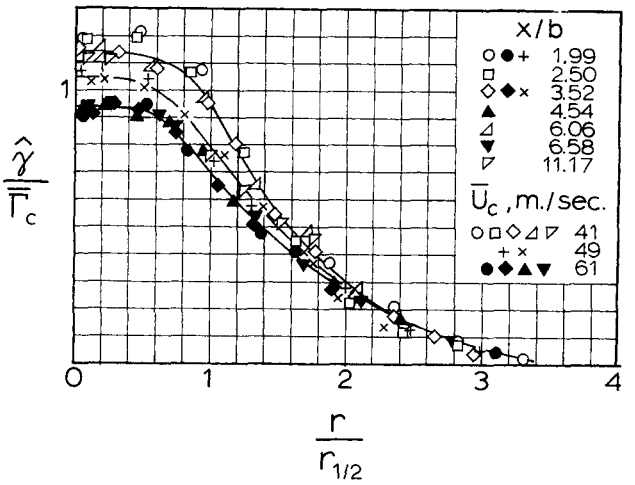

Fig. 6. Radial profiles of the intensity of point concentration fluctuations.

distribution near the plume axis will take the form of the normal distribution.

In the case of a radially constant mean velocity, the material flux through any cross section of the diffusion plume is

$$\bar{U}_c \int_0^\infty \bar{\Gamma} d(\pi r^2) = J \qquad (12)$$

It is therefore expected for the present case that the product $\bar{\Gamma}_c r_{1/2}^2$ should be essentially constant. Table 2 confirms this expectation.

The Spectrum of Point Concentration Fluctuations

The mean-square concentration fluctuation at a point may be decomposed into contributions from different frequencies according to the relation

$$\overline{\gamma^2} = \int_0^\infty E_{\gamma 1}(k_1)\, dk_1 \qquad (13)$$

where $E_{\gamma 1}(k_1)$ is the one-dimensional wave number spectral density function and $k_1 \equiv 2\pi f/\bar{U}$ is the wave number.

Spectral analyses were carried out at a pipe Reynolds number of 450,000 for points on the plume axis 2, 7, and 11 pipe radii from the source. The volume optically probed is of necessity rather large, approximately 1.5 mm. in diameter and due corrections (*15*) were made to obtain the true point concentration fluctuation spectrum. Eddies of the probe's dimension correspond to $bk_1 \simeq 400$. At high wave numbers, the information content of the signal was obliterated by the shot noise associated with the photocathode current. Figure 5 shows the spectra obtained. The trend toward simplification of spectrum shape with increasing distance from the source might be expected on the grounds of a tendency towards equilibrium. The −5/3 power variation of spectral density with wave number expected at high wave numbers for an equilibrium convection subregime is approximated, but the data do not really extend to warrant a conclusion. The trend in the shapes of the spectra is opposite to that found by Lee and Brodkey (*10*) for the diffusion of dye in water, but the significance of this difference is uncertain. Their optical probe though smaller in actual size than the probe used in the present investigation was nearly twice as large in relative size compared to the diameter of the pipe (1-mm. probe in a 75-mm. pipe for their apparatus compared to about 1.5-mm. in 200-mm. for ours).

From the intercept at zero wave number, the integral spatial scale of the concentration fluctuations can be estimated:

$$\Lambda_\gamma = (\pi/2)\, E_{\gamma 1}(k_1 = 0)\, \overline{\gamma^2} \qquad (14)$$

The scales calculated are $\Lambda_\gamma = 0.081\ b$ at $x = 2\ b$; $0.10\ b$ at $7\ b$, and $0.11\ b$ at $11\ b$. These values are of similar magnitude with that found for the Lagrangian scale, $\Lambda_L = 0.084\ b$.

It should be noted that the values quoted for Λ_γ are about appropriate to the case of a molecular Schmidt number $\mu/\rho\mathcal{D}_M$ of approximately unity (realized physically in the case of gas mixing): In using Equation (13) for the calculation of $E_{\gamma 1}(0)/\overline{\gamma^2}$, the spectral density function was assumed to follow a −5/3 power law at high wave numbers. A material such as oil fog has, however, an exceedingly high molecular Schmidt number, that is, the fog particles diffuse Brownianly with the extremest sloth. In this case the spectrum should exhibit a very broad (−1) power region at high wave numbers (*20*), leading to very much higher values of $\overline{\gamma^2}$ and very much lower values of Λ_γ than those presently found. The very high wave number end of the oil fog diffusion spectrum is, of course, experimentally inaccessible, for the material eddies small enough to be affected by Brownian diffusion are microscopic in size. In relation to mixing in liquids, it would be interesting to penetrate the high wave number end sufficiently to fix the beginning of the (−1) power regime. A much smaller light probe than was practicable for the present work would be needed, however.

The Intensity of Point Concentration Fluctuations

A complete mapping was made of the intensity of concentration fluctuations in the diffusion plume. As already implied in the discussion of the spectrum, the use of a

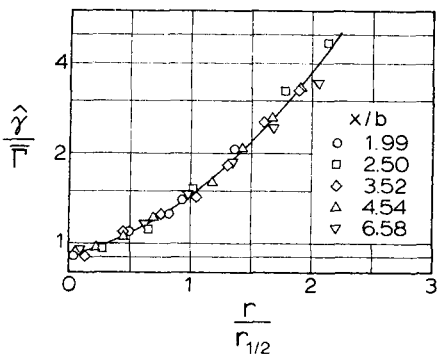

Fig. 7. Radial profiles of the relative intensity of point concentration fluctuations at a Reynolds number of 684,000 (centerline velocity 61 meters/sec.).

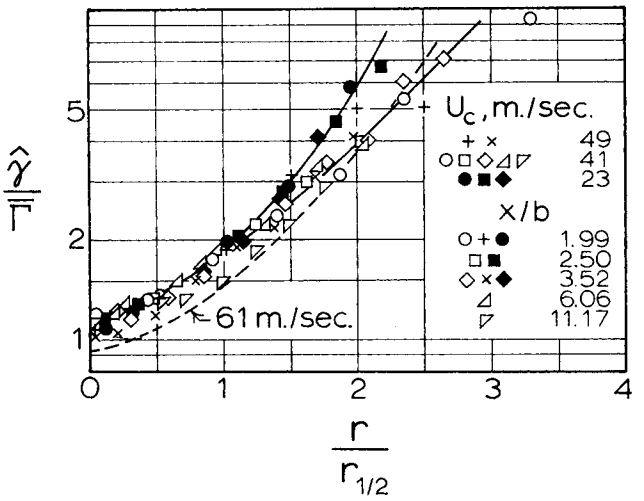

Fig. 8. Radial profiles of the relative intensity of point concentration fluctuations.

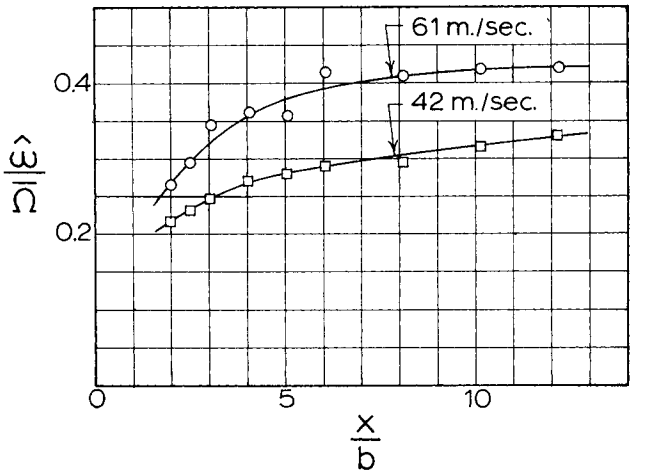

Fig. 9. The relative intensity of cross-sectional concentration fluctuations as a function of distance from the source.

rather large light probe caused a cutoff in response at fairly low wave numbers, in consequence of which the measured intensities give a picture of gas, not oil fog, diffusion, that is, the case of a molecular Schmidt number on the order of unity is portrayed.

Figure 6 shows the intensity data in the form of the normalized profile

$$\hat{\gamma} = \bar{\Gamma}_c \, h(r/r_{1/2})$$

where $r_{1/2}$ is the mean-concentration half-radius. The profiles appear to be self-preserving; there is no visible change with downstream position. There is, however, a definite tendency for the intensity to decrease with increasing Reynolds number (the centerline velocity of 61 meters/sec. corresponds to a Reynolds number of 684,000).

Figures 7 and 8 show the data with the intensity expressed as a fraction of the local mean concentration

$$\hat{\gamma} = \bar{\Gamma} \cdot j \, (r/r_{1/2})$$

a ratio usually spoken of as the relative intensity of fluctuation. It is seen that the relative intensity, already very high on the plume axis, increased rapidly with radial distance. The value of approximately unity on the axis may be compared with the value of about 0.25 attained in turbulent jets (*12, 13*).

The shapes of the profiles seen in Figure 6 are quite similar to those obtained by Lee and Brodkey (Figure 6 of reference *10*) for the diffusion of dye in water. The ratio of fluctuation amplitude to mean concentration that we find, however, is six times as high.

The Intensity of Cross-Sectional Concentration Fluctuations

The term *cross-sectional concentration* refers to the quantity

$$\Omega \equiv \int_0^{2\pi} \int_0^{\infty} \Gamma \cdot r \cdot dr \cdot d\phi \qquad (15)$$

since $\Omega \cdot dx$ is the quantity of material in a sheet of thickness dx is the material density in one dimension of space, a type of one-dimensional concentration.

The time-mean and fluctuating components of Ω are

$$\bar{\Omega} = \int_0^{\infty} \bar{\Gamma} \, d(\pi r^2) \qquad (16)$$

and

$$\omega \equiv \int_0^{2\pi} \int_0^{\infty} \gamma \, r \, dr \, d\phi \qquad (17)$$

The mean-square value of the cross-sectional concentration fluctuations depends on the two-point spatial correlation of point concentration fluctuations. To develop this relation very simply, write

$$\omega \equiv \int_A \gamma \, dA \qquad (18)$$

where dA is an area element in the domain A of material presence in the plume cross section of interest. Then

$$\overline{\omega^2} = \overline{\left(\int_A \gamma \, dA \right)^2} = \int_A \int_A \overline{\gamma' \gamma} \, dA' \, dA \qquad (19)$$

where $\overline{\gamma' \gamma}$ is the correlation between the concentration fluctuations occurring in the area elements dA and dA'.

Figure 9 shows the relative intensity of cross-sectional concentration fluctuations in the diffusion plume as a function of distance from the source. The relative intensity increases at a decreasing rate with downstream distance, tending (as should be expected) toward an equilibrium value. There is a surprisingly large dependence on the mean flow velocity, and the direction of change is opposite to that exhibited by the point concentrations (see Figure 6). Because of the oddness of this result, the data were carefully verified. It would appear from the trends exhibited that the point concentration fluctuations at large separation distances were more highly correlated at the higher flow velocity.

The Spectrum of Cross-Sectional Concentration Fluctuations

The cross-sectional concentration fluctuations can be decomposed into contributions from different frequencies or wave numbers:

$$\overline{\omega^2} = \int_0^{\infty} W(k_1) \, dk_1 \qquad (20)$$

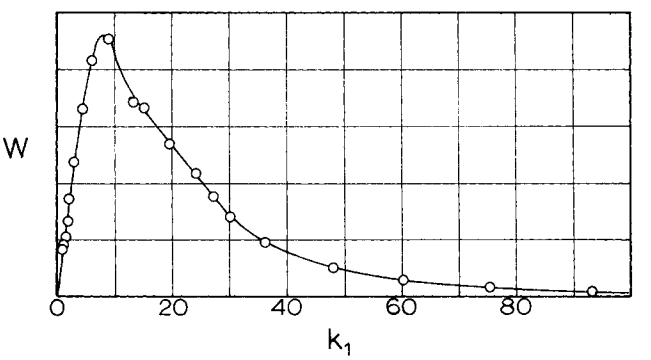

Fig. 10. A typical spectrum of cross-sectional concentration fluctuations.

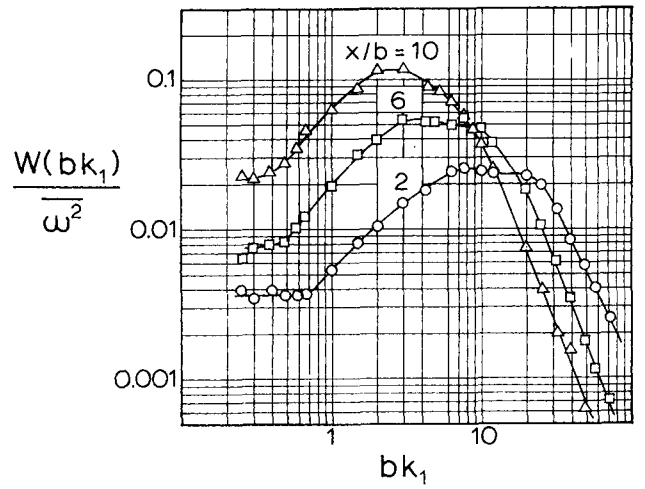

Fig. 11. Spectra of cross-sectional concentration fluctuations at a Reynolds number of 684,000 (centerline velocity 61 meters/sec.).

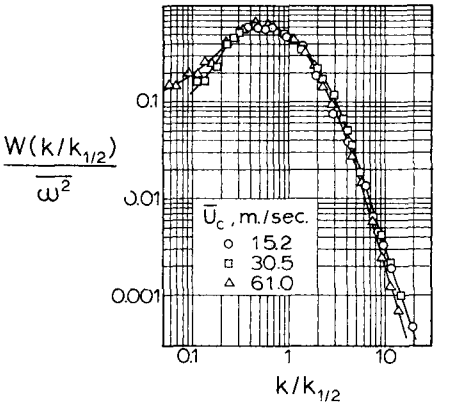

Fig. 13. Spectra of cross-sectional concentration fluctuations in a section far from the source ($x = 12.2\ b$).

where $W(k_1)$ is the spectral density function and $k_1 \equiv 2\pi f/\bar{U}_c$ is the wave number. Since Ω and ω reflect a two-dimensional sampling of a three-dimensional space $W(k_1)$ should reflect more directly than $E_{\gamma 1}(k_1)$ the distribution of material eddies in the diffusion plumes. In particular, there should appear to be few eddies of very large diameter and so the spectrum should be distinctly humplike in shape.

The cross-sectional concentration fluctuations were spectrally analyzed at several downstream distances and flow velocities. Figures 10 and 11 confirm the general expectation as to the spectrum shape. But the significance of the low-level plateau apparent in Figure 11 at very low wave numbers is uncertain. Figures 11, 12, and 13 show that the spectra tended toward a simple limiting form at sections far from the source—a featureless hump, nearly symmetrical in a log-log representation. Near the source, variations in mean velocity produced considerable change, Figure 12, but the effect diminished with downstream distance, Figure 13. The differences between the spectra in Figure 13 are within the experimental error.

In order to afford a clear comparison of the spectral shapes for the limiting regime far from the source, the data in Figure 13 are shown in the normalized form

$$W = \overline{\omega^2}\, W(k_1/k_{1/2}) \tag{21}$$

where $k_{1/2}$ is the centroid of the spectrum:

$$\overline{\omega^2}/2 = \int_0^{k_{1/2}} W(k_1)\, dk_1 \tag{22}$$

Now the reciprocal of the wave number is identified with eddy size; hence $(k_{1/2})^{-1}$ is an average measure of the spatial scale of the eddies affecting most the value of $\overline{\omega^2}$. Figure 14 shows the dependence of this scale on distance from the source. The irregularity of the data probably has little general significance: First, the possible error in estimating $k_{1/2}$ was fairly large, and second, a somewhat erratic behavior is not altogether unexpected for the large eddies dominating the composition of $\overline{\omega^2}$. What can be conclusively said is that $(k_{1/2})^{-1}$ is of similar magnitude with the plume half-radius (compare Figures 3 and 14).

The reciprocal k_m^{-1} of the wave number at which the maximum of the spectral density function occurs is another measure of average eddy size, more poorly defined than $(k_{1/2})$. This scale is shown as a function of downstream distance in Figure 15.

CONCLUSION

The nearly homogeneous, isotropic turbulence field in the core of a fully developed pipe flow was chosen as the medium for turbulent dispersion of a smoke tracer injected from a point on the centerline. By using the optical probe technique the fields of the mean and fluctuating point concentration were mapped at several Reynolds numbers, and spectral analyses were made of concentration fluctuations on the plume axis. With the use of sheet illumination, measurements were also made of the mean and fluctuating components of the integral material

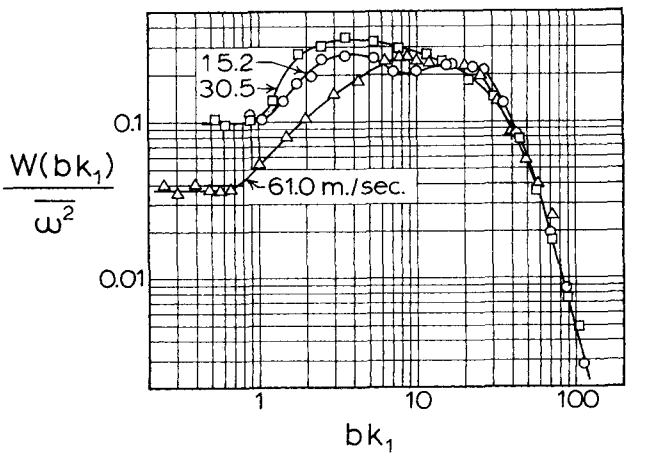

Fig. 12. Spectra of cross-sectional concentration fluctuations in a section near the source ($x = 1.99\ b$).

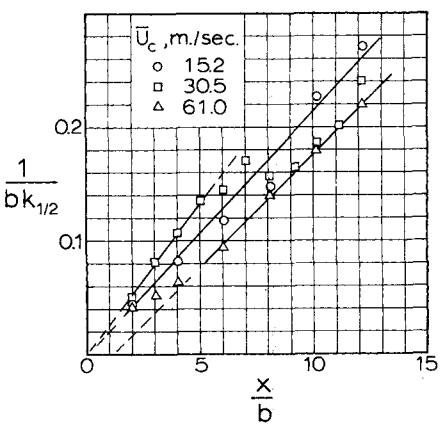

Fig. 14. Relation between the centroid ($k_{1/2}$) of the $\overline{\omega^2}$ spectrum and distance from the source.

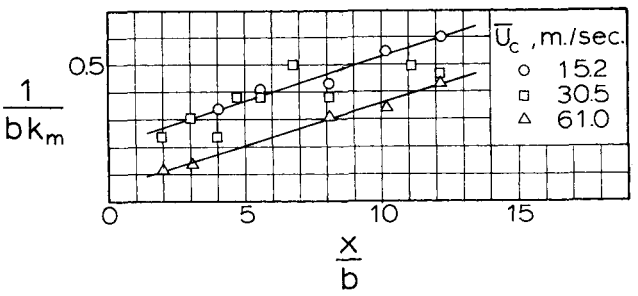

Fig. 15. Relation between the maximum point (k_m) of the $\overline{\omega^2}$ spectrum and distance from the source.

concentration in a plume cross section, and the fluctuating component was spectrally analyzed. The maximum Reynolds number was 684,000, the maximum ratio of root-mean-square concentration fluctuation to mean concentration exceeded 100% for points and 40% for sheets, and the turbulent Peclet number was found to equal 850. The existence of standard flow conditions was confirmed by measurement of the frictional drag coefficient and the mean concentration field.

The experimental data presented here refer, of course, to the dispersion of colloidal size matter into a gaseous environment. It is of interest to note that Wilson and Danckwerts (*22*) have recently demonstrated experimentally that somewhat different results are obtained if gases are used to simulate the mixing of liquids, or vice versa, in model experiments while background information dealing with the relationship of fog scattered light measurements to the mixing for a normal gas system has been given in references *12* and *13*. It is expected, following consideration of the experimental and theoretical size of the eddies, the dimensions of the optical probe, the molecular diffusivity of air, the Brownian diffusivity of fog particles, and the theoretical equations of motion and matter conservation when examined for conditions of similitude, that the present measurements obtained with a finite size probe correspond closely to measurements that would be obtained with a probe with excellent response in detecting the mixture of one air stream (imagined tagged) with another.

ACKNOWLEDGMENT

The research was sponsored by the Air Force Cambridge Laboratories of the Office of Aerospace Research under contract AF19(604)-6181. The present paper is based on the final report numbered AFC RL-63-727.

The kindness of Professors H. C. Hottel and G. C. Williams in making the facilities of the Massachusetts Institute of Technology Fuels Research Laboratory available for the investigation is gratefully acknowledged.

NOTATION

The instantaneous values of statistically steady turbulently fluctuating quantities are in this paper denoted by capital letters. The time-mean value (indicated by an overbar) of such a quantity W is

$$\overline{W} \equiv \lim_{T\to\infty} \frac{1}{T}\int_t^{t+T} W\,dt$$

The fluctuations of such quantities are denoted by lower case letters, for example, $w \equiv W - \overline{W}$. The mean-square amplitude of a fluctuation w is

$$\overline{w^2} \equiv \lim_{T\to\infty} \frac{1}{T}\int_t^{t+T} w^2\,dt$$

The root-mean-square amplitude (indicated by the oversign $\wedge$) follows as $\hat{w} \equiv \sqrt{\overline{w^2}}$. The root-mean-square amplitude of fluctuation is commonly called the intensity of fluctuation.

b = pipe radius
C = correlation coefficient for point concentration fluctuations at two points in space
c = centerline value
D_p = pipe diameter
$\mathcal{D}_T$ = turbulent diffusivity
$E_1(k_1)$ = spectral density function for point concentration fluctuations
f = frequency
J = source strength (source material flux)
K = correlation coefficient for concentration fluctuations occurring in two plume cross sections
k_1 = wave number ($\equiv 2\pi f/U$)
M = molecular diffusivity
m = maximum
N_{Pe} = turbulent Peclet number ($\equiv D_p\overline{U}_c/\mathcal{D}_T$)
N_{Re} = pipe Reynolds number ($\equiv D_pU_{av}\,\rho/\mu$)
$\overline{r^2}$ = mean-square material displacement radius of plume
$r_{1/2}$ = concentration half-radius of plume
U = axial x component of velocity
U_{av} = average flow velocity through pipe (discharge divided by area)
v = radial component of turbulent velocity fluctuation
$W(k_1)$ = spectral density function for cross-sectional concentration fluctuations
$\overline{y^2}$ = mean-square y component of material displacement from the time-mean center of gravity ($\overline{y^2} = \frac{1}{2}\,\overline{r^2}$ here)
$\overline{Y^2}$ = mean-square y component of material displacement from the instantaneous center of gravity
$\overline{Y^2}_o$ = mean-square y component of the displacement of the instantaneous center of gravity from the time-mean center

Greek Letters

Γ = point concentration
γ = point concentration fluctuation
ζ, η = distance of separation between pairs of points in space
Λ_L = Lagrangian scale of turbulence
Λ_γ = integral spatial scale of point concentration fluctuations
Λ_ω = integral spatial scale of cross-sectional concentration fluctuations
μ = viscosity
ρ = density
Ω = cross-sectional concentration
ω = cross-sectional concentration fluctuation

LITERATURE CITED

1. Brier, G. W., *J. Meteorol.*, **7**, 283 (1950).
2. Gifford, F., "Advances in Geophysics," Vol. 6, Academic Press, New York (1959).
3. Taylor, G. I., *Proc. London Math. Soc.*, **20**, 196 (1921).
4. Richardson, L. F., *Proc. Royal Soc. (London)*, **A110**, 709 (1926).
5. Lin, C. C., *Proc. Natl. Acad. Sci.*, **46**, 566, 1147 (1960).
6. Hinze, J. O., "Turbulence," McGraw-Hill, New York (1959).
7. Stommel, H. M., *J. Marine Res.*, **8**, 199 (1949).
8. Hutchings, J. W., *J. Meteorol.*, **12**, 263 (1955).
9. Corrsin, Stanley, and M. S. Uberoi, *Natl. Advisory Committee Aeronaut. Rept. No. 1040* (1951).

10. Lee, J. L., and R. S. Brodkey, *A.I.Ch.E. J.*, **10**, 187 (1964).
11. Rosensweig, R. E., Sc.D. thesis, Massachusetts Inst. Technol., Cambridge (1959).
12. ———, H. C. Hottel, and G. C. Williams, *Chem. Eng. Sci.*, **15**, 111 (1961).
13. Becker, H. A., Sc.D. thesis, Massachusetts Inst. Technol., Cambridge (1961).
14. ———, H. C. Hottel, and G. C. Williams, paper presented at Ninth Symp. (International) on Combustion (1962).
15. ————————, paper presented at A.I.Ch.E. Houston meeting (Dec., 1963).
16. Baldwin, L. V., and T. J. Walsh, *A.I.Ch.E. J.*, 7, 53 (1961).
17. Flint, D. I., Hisao Kada, and T. J. Hanratty, *ibid.*, **6**, 325 (1960).
18. Mickelson, W. R., *Natl. Advisory Committee Aeronaut. Tech. Note 3570* (1955).
19. Towle, W. L., and T. K. Sherwood, *Ind. Eng. Chem.*, **31**, 457 (1939).
20. Batchelor, G. K., *J. Fluid Mech.*, **5**, 113 (1959).
21. Forslund, R. P., and H. B. Sargent, "Influence of Reynolds Number on Mixing in Turbulent Free Jets," Linde Speedway Res. Lab., Indianapolis, Ind. (1961).
22. Wilson, R. A. M., and P. V. Danckwerts, *Chem. Eng. Sci.*, **19**, 885 (1964).

Manuscript received December 9, 1965; revision received March 21, 1966; paper accepted March 30, 1966. Paper presented at A.I.Ch.E. Boston meeting.

Hydrodynamics of Rivulet Flow

G. D. TOWELL and L. B. ROTHFELD

Shell Development Company, Emeryville, California

A theoretical analysis of the hydrodynamics of liquid rivulets flowing down an inclined surface is presented. Steady state solutions are developed for the laminar flow case which relate the flow rate to the rivulet width, the physical properties of the liquid, and the contact angle. Excellent verification of the theoretical predictions was obtained in a number of experiments with various liquids on an inclined glass plate. All constants in the equations were derived from theory. These results will be useful in obtaining a better understanding and correlation of such phenomena as liquid flow over packings and catalysts and flow along walls and tube surfaces, as in condensation and evaporation.

When a liquid flows down an inclined surface at a low rate, separate rivulets form instead of a continuous film. This is an important phenomenon in the operation of packed contactors where packings are used to distribute the liquid; trickle phase reactors where the liquid is distributed over a catalyst; and in condensation and evaporation on surfaces.

The objective of this work is to study theoretically and experimentally the hydrodynamics of rivulet flow on an inclined flat surface. (The contiguous gas phase is stationary.) Steady state theoretical solutions are developed for the laminar flow situation which is a realistic one over a wide range of rivulet flow rates. A reduced form of the Navier-Stokes equations is solved with special boundary conditions of a finite contact angle at the edge of the rivulet and relations between the pressure inside and outside a curved interface. The shape of the interface and the velocity profile in the rivulet are obtained, and an integration of this velocity profile gives a relation between the rivulet width and the flow rate. This relation contains the plate inclination; the contact angle of the liquid on the plate; and the fluid properties, viscosity, density, and surface tension.

Experiments were carried out over a wide range of flow rates with a variety of liquids on a glass plate at different inclinations. Measurements of rivulet width as a function of flow rate were made in the region where the rivulet had attained steady state. Optical measurements were made of the contact angle on the edge of the actual moving rivulet. The experimental values of the rivulet width were compared with theoretical values computed from the measured flow rate and contact angle. Above a certain flow rate waves appeared on the film and observations were made of the incidence and character of these waves.

THEORY

Development of Flow and Interface Equations

The problem of describing theoretically the flow of a rivulet entails two aspects: the description of the gas-liquid interface and the calculation of the velocity distribution. The theory developed below considers only that portion of the stream which has traveled far enough so that the shape of the cross section no longer changes along the stream path. The flow is then considered to be one dimensional, with a velocity component only in the direction of the stream. Since acceleration effects are neglected, the equations of motion (Navier-Stokes equations) sim-

L. B. Rothfeld is with Shell Oil Company, Deer Park, Texas.